Technical Note	**1966-54**
A Preliminary Study of Klystron Distortion in a CHIRP Radar System	H. M. Heggestad 28 December 1966

Lincoln Laboratory

MASSACHUSETTS INSTITUTE OF TECHNOLOGY

Lexington, Massachusetts
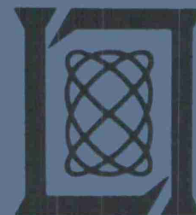
MASSACHUSETTS INSTITUTE OF TECHNOLOGY

LINCOLN LABORATORY

A PRELIMINARY STUDY OF KLYSTRON DISTORTION
IN A CHIRP RADAR SYSTEM

H. M. HEGGESTAD
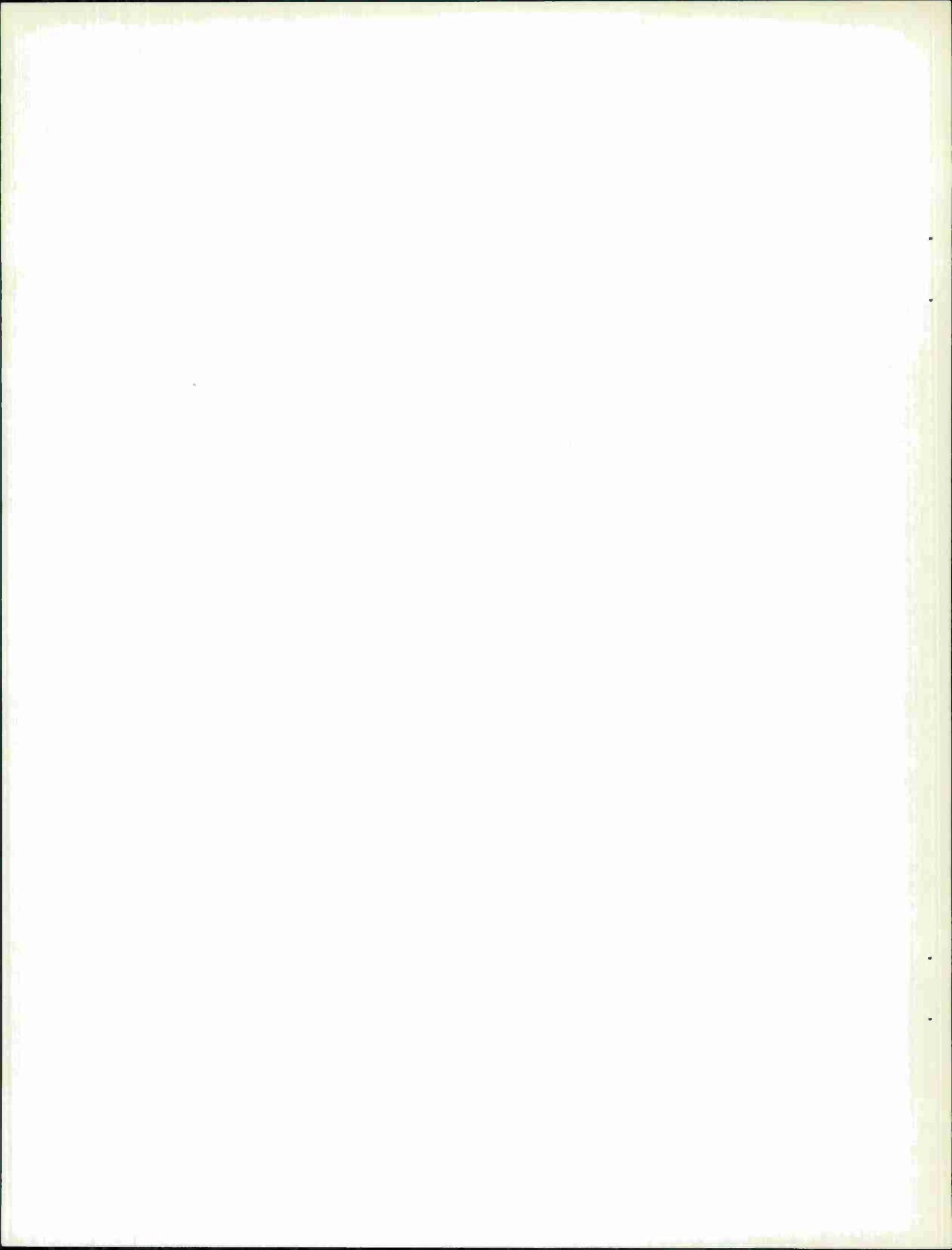
Group 42

TECHNICAL NOTE 1966-54

28 DECEMBER 1966

LEXINGTON   MASSACHUSETTS

ABSTRACT

A study has been made of the effects of klystron saturation, and phase and amplitude distortion, on the performance of a wideband high-power CHIRP radar system. Mathematical analysis of a general non-linear model for a klystron indicates that satisfactory operation of the radar system can still be achieved in the face of the grossly non-ideal character of the tube, with suitable restrictions, if appropriate compensation is applied. Extraneous paired echoes in the signal at the klystron input (whether present because of previous distortion, or deliberately introduced by a transversal equalizer) are shown to have a specific relationship with paired echoes at the klystron output.

A FORTRAN computer program has been written to simulate the performance in a CHIRP system of any suitable klystron (or other high-power amplifier tube, such as a twystron or TWT). The inputs to the program include measured tube data, such as the CW amplitude versus frequency and phase versus frequency characteristics and the input versus output saturation curve. The user of the program specifies what he feels is the useable bandwidth of the tube. The program simulates a pure CHIRP signal of that bandwidth and delivers plots of the weighted compressed pulse that would appear at the receiver output.

In addition, by inspection of the output compressed pulse plots, one can estimate transversal equalizer settings to cancel the spurious sidelobes, introduce the equalized CHIRP pulse into the program in place of the former undistorted input, and observe the degree of compensation in the output pulse.

The report includes reproductions of the output plots generated by the simulation program, for a representative set of klystron data.

TABLE OF CONTENTS

A Preliminary Study of Klystron Distortion in a CHIRP Radar System

I. INTRODUCTION

The development of modern wideband high-power klystron tubes has placed heavy emphasis on optimization of bandwidth, pass band flatness, and output power, with relatively little regard for linearity of the phase versus frequency characteristic. For applications in which a constant-frequency pulse is transmitted this factor need not be considered. For a CHIRP radar system, however, any deviations from phase linearity (and/or amplitude flatness) give rise to spurious time sidelobes, degrading the performance of the system.

In undertaking the design of a wideband high-power CHIRP radar it has become apparent that, if an existing klystron is to be used, its phase and amplitude distortion will be primary contributors to time sidelobes in the received signal. Thus there arises the problem of predicting the performance in a CHIRP system of available klystrons (as well as other devices, such as twystrons and traveling wave tubes), with the two-fold objective of a) aiding in selection of the best tube type, and b) studying the problem of compensating the distortion introduced by the tube.

The general goal of the present work is pragmatic in nature: a mathematically tractable non-linear model is devised, which can be fitted to measured characteristics of an actual klystron, and applied to the specific problem of analyzing klystron behavior in a CHIRP radar. The model is useful over a reasonable range of operating conditions, and is sufficiently general to permit application to many different tubes. Some preliminary calculations were performed (see Appendix B) to determine the effects of a general soft-limiting phase- and amplitude-distorted device upon a CHIRP signal; the detailed information about specific tubes, however, is generated by a fairly complex computer simulation, as described in succeeding sections.

One of the most interesting results of the work is definite indication that, with suitable restrictions, a transversal equalizer preceding a klystron can effectively cancel much of the tube's distortion.

1

II. SIMULATION ALGORITHM

A. Philosophical Considerations

One may imagine many types of measurements to make upon a klystron, each valid over a more or less restricted operating range, such as

1. amplitude versus frequency (which is a function of drive level, beam voltage, and filament current)
2. phase versus frequency (also a function of drive, beam and filament operating levels)
3. the non-linear input versus output characteristic, or saturation curve (which varies somewhat with frequency)
4. the non-linear coupling between input amplitude and output phase (also a function of frequency)

All of these measurements are presumed to be made at a series of discrete frequencies, with pulsed CW. In utilizing this data in a model to be used with a CHIRP signal, one must adopt the point of view that the signal is actually CW, with a slowly-varying center frequency; as a matter of fact, the sawtooth plot of frequency versus time for a typical radar CHIRP signal is much narrower-band than the other attributes of the signal.

The operating-point dependence of the tube's characteristics could surely be reflected by a sufficiently complex model. Regarding the tube as part of an operational system, however, in which tube and signal parameters are fixed, the approach here has been to take tube data over some sort of "average" operating region, assuming that the variations in question would contribute only to second-order effects.

The critical problem in specification of the model was selection of its components, and their relative locations. Clearly linear filters could be used to represent the measured phase and frequency distortions; their effects can be handled nicely by means of paired-echo theory (see Appendix A). An attractive option for representing tube saturation is a linear-phase frequency-independent soft limiter, both for analytic calculations (see Appendix B) and for the computer algorithm. The dilemma, however, is in deciding the locations of these devices relative to each other. The three possibilities are diagrammed in Fig. 1.
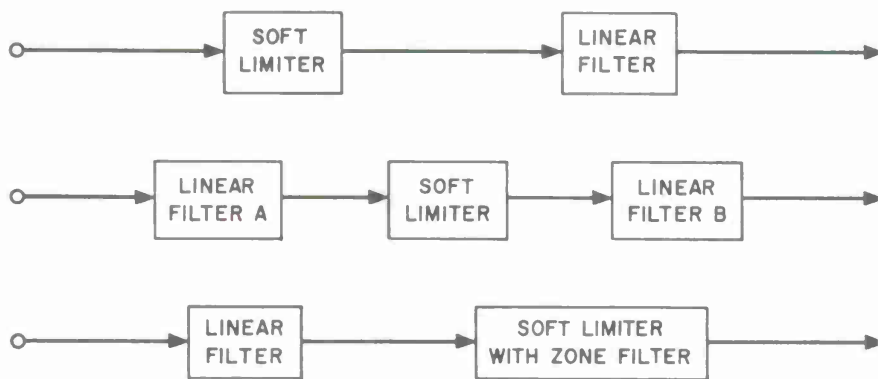
Fig. 1.   Alternative configurations of core of klystron model.

3

There is no prima facie evidence to indicate which scheme corresponds to the actual process in a klystron (if, indeed, the phenomena occur in discrete steps). The first diagram is clearly unsatisfactory, since a constant-amplitude pure CHIRP signal applied to it would simply be attenuated by the limiter, with the result that the klystron model would be nothing more than a linear filter. For the second diagram, which is probably more realistic, it is impossible to determine by external measurements how the true phase and amplitude distortion should be distributed between filter A and filter B. In the interest of simplicity, therefore, it was decided for present purposes that filter B should be simply an ideal low-pass (or "zone") filter, to suppress the harmonics generated by the ideal soft limiter. If the zone filter is regarded as combined with the limiter, one has the configuration in the third diagram.

The effects of the non-linear coupling between input amplitude and output phase are discussed analytically in Appendix B. The initial version of the computer simulation does not include this effect, although it can be added with relative ease.

In view of the foregoing comments, it should be clear that results obtained with this model must be interpreted with due regard for their approximate nature. An attempt has been made to balance precision of the representation against complexity and computer running time, with the objective of obtaining insight and quasi-quantative data on klystron operation in a CHIRP radar.

B.   Description of Simulation Algorithm

The computer mechanization of the problem is basically equivalent to generating a distorted transmitted pulse using the klystron model, receiving a noiseless replica of it, and processing the received signal in a rudimentary "STRETCH" receiver, whose output is a plot of the weighted compressed pulse with distortion-induced spurious time sidelobes. The TW product of the CHIRP signal is taken to be very large, permitting the usual simplifying approximations.

The following block diagram presents the skeleton of the algorithm:

CHIRP AT FREQUENCY
$(f_c - f_{if})$

-42-10220

CHIRP AT
FREQUENCY f_c → | LINEAR FILTER | → | IDEAL SOFT LIMITER | → | CORRELATION MIXER | → | IDEAL LOW-PASS FILTER | → | 40 db WEIGHTING | → | SPECTRUM ANALYSIS | → OUTPUT
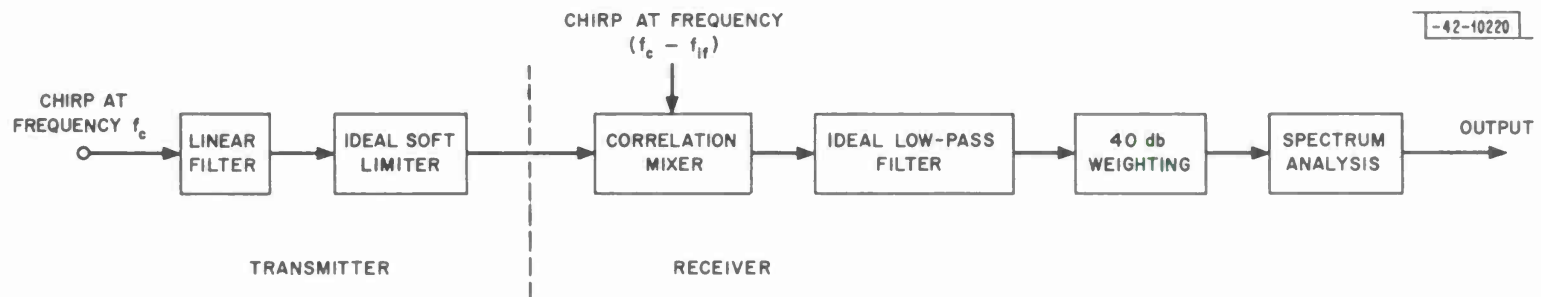
TRANSMITTER   RECEIVER

Fig. 2.   Basic block diagram of simulation algorithm.

The linear filter in Fig. 2 represents the resultant (through the fifth harmonic) of the Fourier components of the actual measured amplitude and phase characteristics of the klystron under consideration. The signal entering the limiter is computed in the program as the sum of a pure CHIRP signal plus leading and lagging echoes corresponding to the Fourier components of the filter characteristics.

The ideal soft limiter in the figure has as its amplitude characteristic the input versus output saturation curve of the klystron, measured at the klystron's nominal center frequency.

The signal entering the correlation mixer consists of the superposition of a distorted CHIRP signal and a number of distorted leading and lagging echoes at the original carrier frequency, as well as components at odd-integral multiples of the carrier frequency (see Appendix B. The soft limiter, an odd-symmetric device, generates odd-order harmonics of the input frequency.) At the output of the ideal low-pass filter following the correlation mixer (which cuts off somewhat above f_{if}, where $f_{if} \ll f_c$), the signal is the superposition of a number of rectangular CW pulses, with center frequencies distributed about f_{if}, corresponding to the main pulse and the paired echoes. (See Appendix C for a description of the computer simulation of the low-pass filter.) The IF signal is the time-domain analog of the spectrum of the distorted CHIRP pulse. When weighted in the time domain and Fourier transformed, the signal becomes the frequency-domain analog of the weighted compressed pulse produced by an ordinary matched-filter CHIRP receiver.

Figure 3 is a simplified flow diagram of the actual FORTRAN program for simulating the klystron, to be explained in more detail in the next section.

C. Program Operation

The user must provide the following data cards:

1. NSAMPL, I10 format - the length of the arrays
    AMPL and PHAS below
2. DELTAF, F12.2 - the frequency interval (MHz)
    between measured data
3. FFIRST, F12.2 - the frequency (MHz) corre-
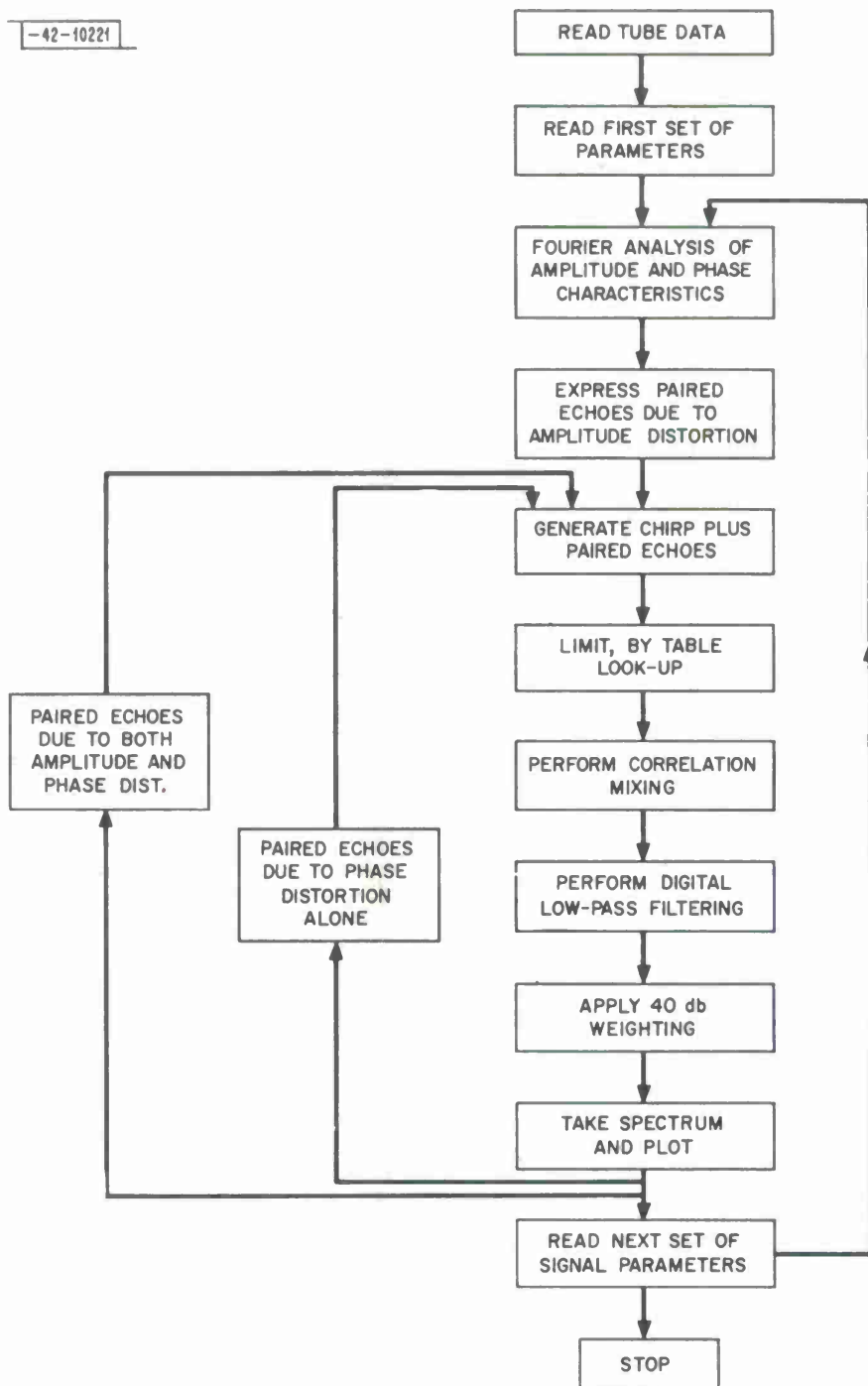   sponding to the first point of array AMPL(I)

Fig. 3. Flow chart of computer program.

4ff.   AMPL(I), 2X, 7F10.2 - as many cards as
        necessary to transmit the NSAMPL values
        of output power versus frequency data

5ff.   PHAS(I), 2X, 7F10.2 - NSAMPL values of
        phase versus frequency data

6.   NSAT, I10 - the number of points in array
        SAT(I) below

7ff.   SAT(I), 2X, 7F10.2 - NSAT values of input
        level versus output level saturation curve
        data

8-13.   First set of signal parameters

8.   NRUN, I10 - the consecutive identifying
        number of the current set of signal
        parameters

9.   EDGE, F12.2 - the value of AMPL at the edge
        of the band specified for the current run,
        as a fraction of the value of AMPL at band
        center

10.   WIDTH, F12.2 - the useable tube bandwidth
        specified for the current run

11.   FLEFT, F12.2 - frequency (MHz) corresponding
        to the point of AMPL at the left-hand edge
        of the selected band

12.   TIME, F12.2 - duration in microseconds of the
        desired CHIRP pulse for the current run

13.   OPPT, F12.2 - value to which input signal
        amplitude is to be normalized (specifies
        the current operating point on the saturation
        curve)

14.   SR, F12.2 - the sampling rate for generation
        of the input CHIRP signal. The value 25,000
        has been found in practice to provide a
        satisfactory balance of accuracy and program
        running time.

8

15-21, 22-28, etc. - the program may be used to investigate as many different signal configurations as desired, each requiring a set of seven data input cards similar to 8-14 above

Last Card in the data deck must have a zero in column 10, which causes the program to terminate

The following comments provide additional explanation and description of the data cards and their implications in the program.

A reasonable value for NSAMPL, to insure accuracy of the simulation, might be on the order of 100 or greater. No upper limit for NSAMPL is specified.

Note that the array AMPL(I) is assumed to be in the form of output <u>power</u> versus frequency. The program converts it to an output voltage characteristic, assuming an impedance of 377 ohms.

The array PHAS(I) must be the "unfolded" phase. The manufacturer's phase data will probably be given modulo 360 degrees, necessitating correction before use of the data in the program. The phase data will have a linear ramp component, in general, which corresponds to a fixed delay. Since fixed delay may be ignored for simulation purposes, but the length of the delay is not known, the program subtracts off the least-mean-square-error ramp from the phase data.

The saturation curve is presumably provided by the manufacturer in the form of a few values of output power versus input power, in the vicinity of the knee of the curve. This data must be manually rescaled (assuming appropriate input and output impedances, which for practical purposes might be taken to be 377 ohms), so that the curve represents output voltage V_o versus input voltage V_{in}, where

    a. V_{in} ranges from 0 to 1, and V_o has about the same range;

    b.   the knee of the curve occurs at about $V_{in} = 0.7$;

    c.   if the original data does not extend all the way down to $V_{in} = 0$, then a straight line is drawn from zero to the first (rescaled) data point;

    d.   if the original data extends beyond the point where the curve acquires negative slope, those data points are replaced by a straight line of zero slope (corresponding to the assumption that the actual operating level never rises much beyond the point of zero slope)

V_{in} must be divided into NSAT equal increments (where NSAT might be 20 or more); the array SAT(I) represents the corresponding values of V_o on the rescaled and modified curve. The first value, SAT(1), is not zero; it corresponds to $V_{in} = 1/\text{NSAT}$.

There are two advantages in performing this relatively simple processing by hand, rather than in the computer: the programming task is substantially simplified, and the matter of selecting the operating point OPPT on the saturation curve is much easier when one has the normalized and rescaled curve at hand.

Presumably the user of the program will have made a rough plot of the raw data of output power versus frequency. By inspection, he will select what he feels is a useable portion of the curve for the first run, thereby determining the values EDGE, WIDTH, and FLEFT to provide on data cards 9, 10, and 11. The program will generate a CHIRP pulse of frequency sweep equal to WIDTH, duration of TIME microseconds, and center frequency equal to the center of the useable band selected by the program user.

Additional sets of six signal parameter cards are to be provided, if the user wishes to investigate other possible specifications of the "useable band" of the tube.

D. Outputs Provided by the Program

In order to decrease quantization error, the members of the input array SAT(I) are spread apart by the program, and connected by straight lines, to approximately fill an array of length 1000. A graph of this modified curve is the first output from the program.

For each run (i.e., for each set of six signal parameter data cards), the following output information is provided:

1. A printed table of the sine and cosine coefficients, to the fifth harmonic, the results of Fourier analyzing the amplitude and phase data

2. A plot of the amplitude curve, reconstructed from the Fourier coefficients, superimposed upon a plot of the original data

10

3. A plot of the input phase data

4. A graph of the fine structure of the phase data,
    after removal of the ramp component, superimposed
    upon its Fourier reconstruction

5. A plot of the 40 db weighted compressed pulse,
    incorporating the effects of the amplitude
    distortion alone

6. A plot of the weighted compressed pulse, when
    only the phase distortion is present

7. A plot of the weighted compressed pulse, showing
    the effects of both amplitude and phase distortion

Should the extra information provided by plots (5) and (6) turn out to have
relatively little value, the computer running time can be reduced by about half
by deleting the program sections leading to these plots.

III. TYPICAL RESULTS

Figures 4 - 10 below are the results of operation of the program with a
set of representative klystron data.

Figures 8,9, and 10, which represent time-domain compressed pulses, have
their x - axes calibrated in frequency, because they are in fact magnitudes of
spectra of rectangular pulses. Their axes should be rescaled to correspond to
the pulse duration T and frequency sweep W of the CHIRP signal (10 µsec and
475 MHz, in this case). Thus the 4 MHz point on these graphs corresponds to
$t = 0$, and the 1 MHz and 7 MHz points correspond to $t = \pm \frac{30}{475}$ microseconds, or
$t \cong \pm 63.2$ nanoseconds, respectively. This rescaling will be made an automatic
feature of the program in the near future.

11
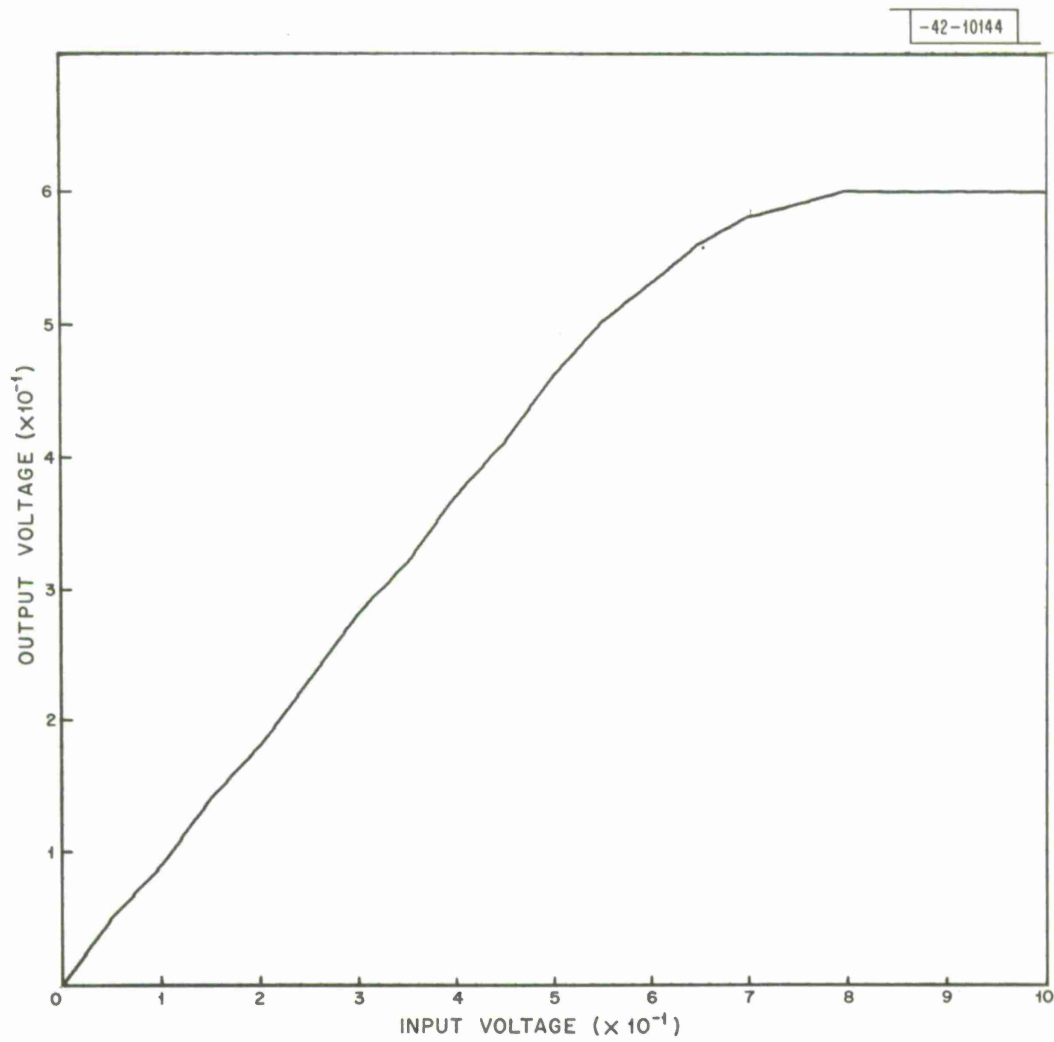
Fig. 4. Saturation curve.

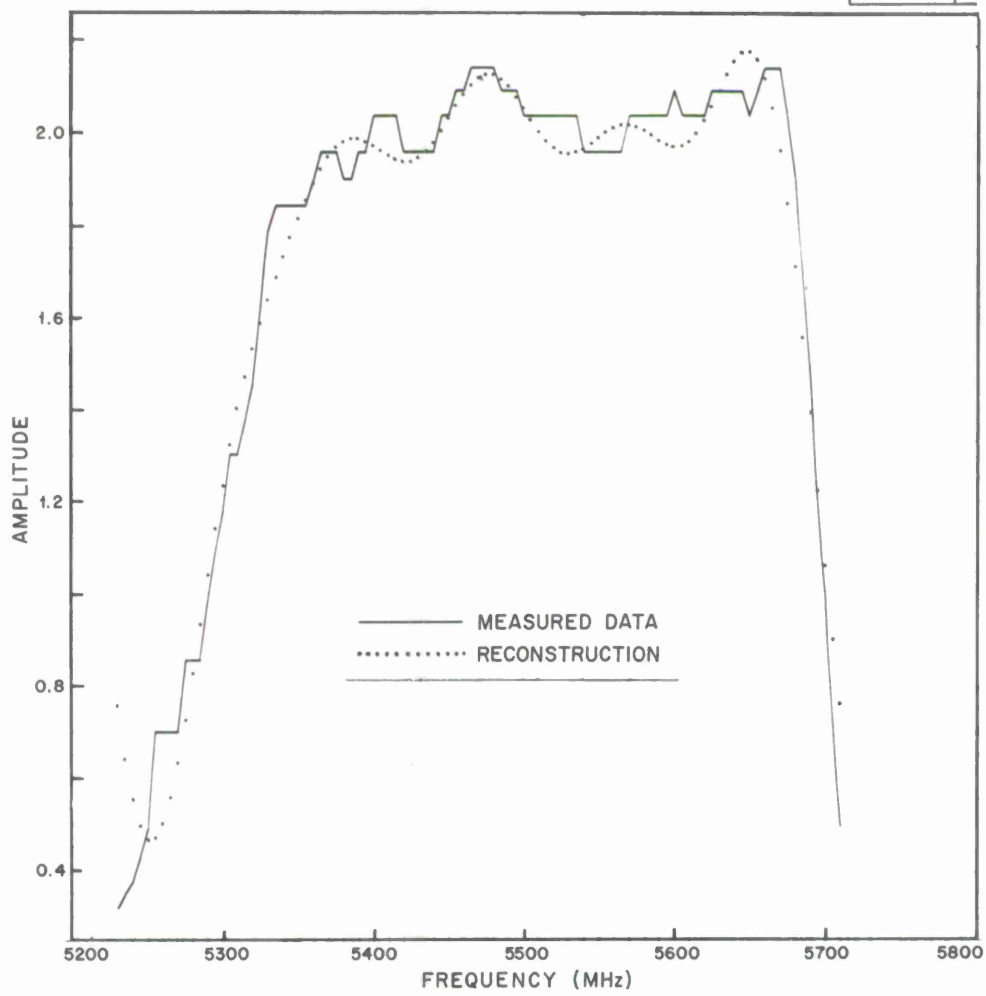Fig. 5. Amplitude versus frequency characteristic.

13
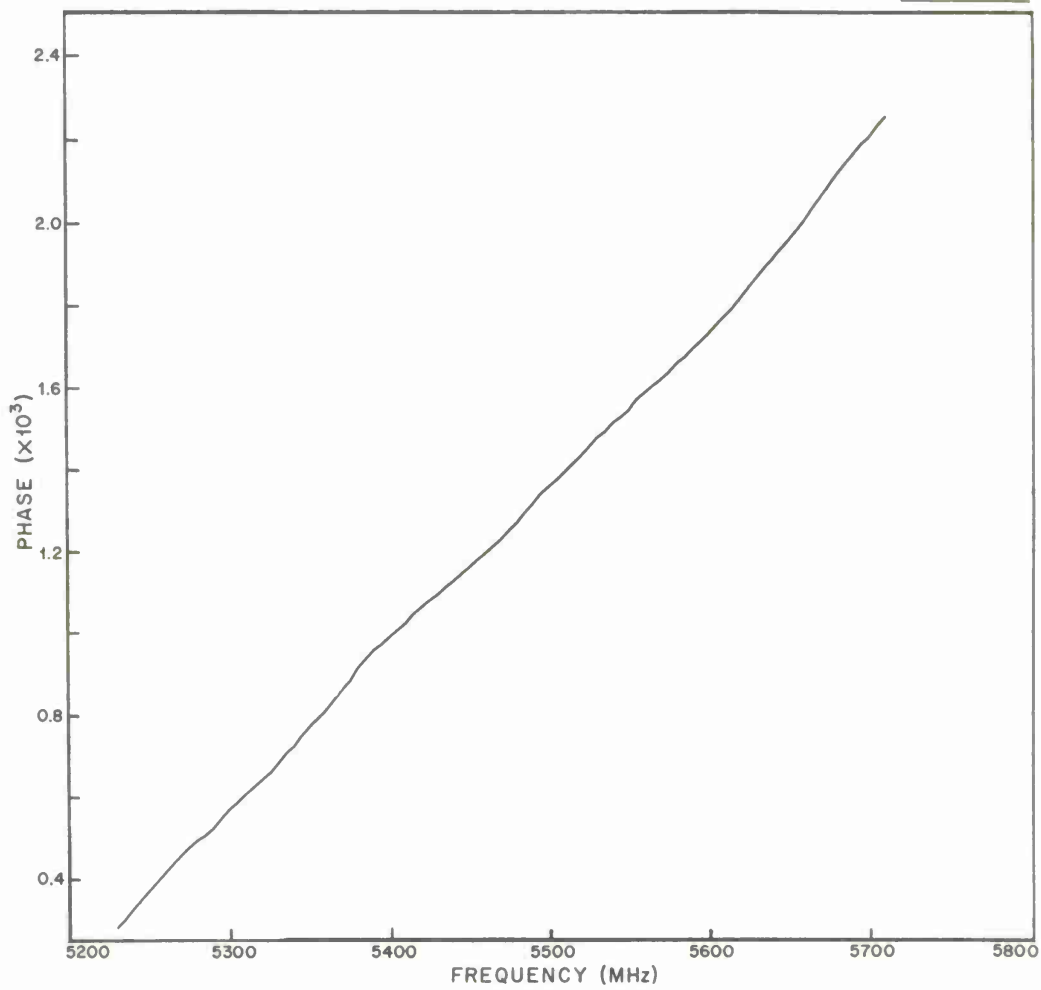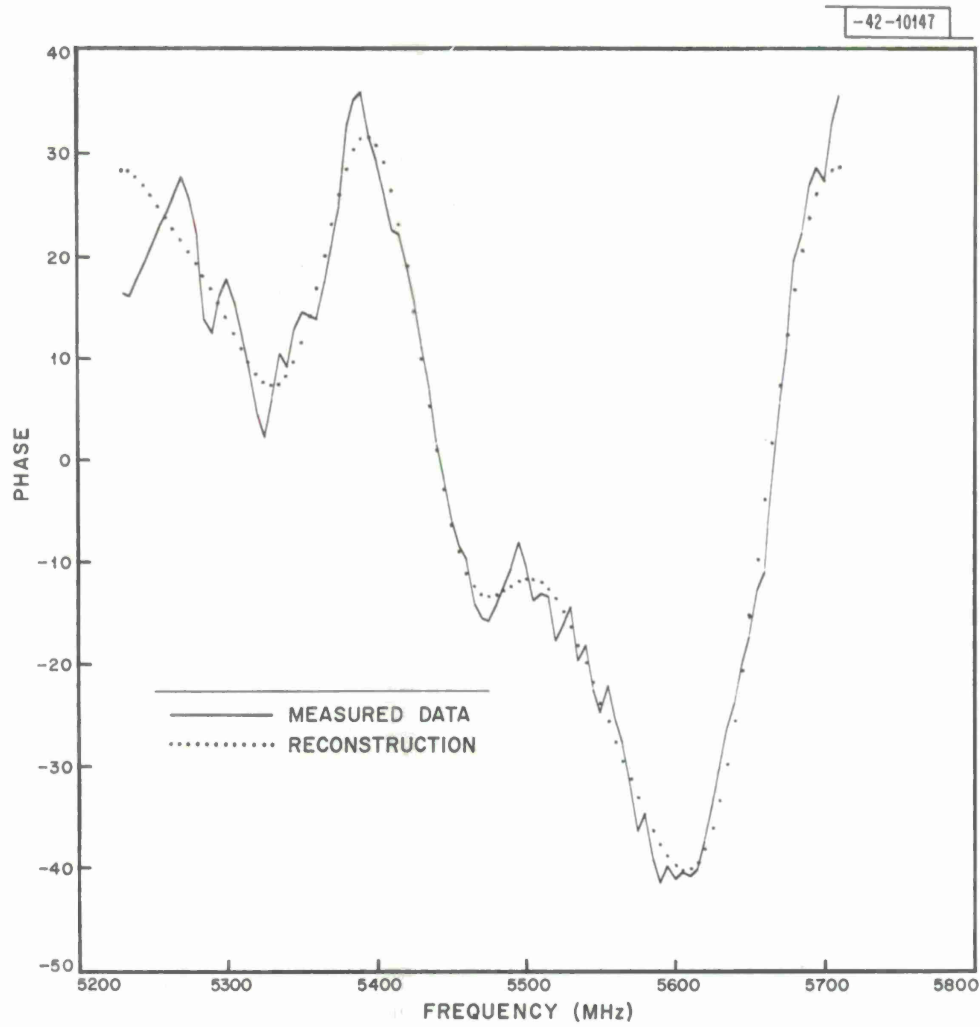
Fig. 6.   Measured phase characteristic.

Fig. 7. Phase characteristic (after subtraction of linear component).

15

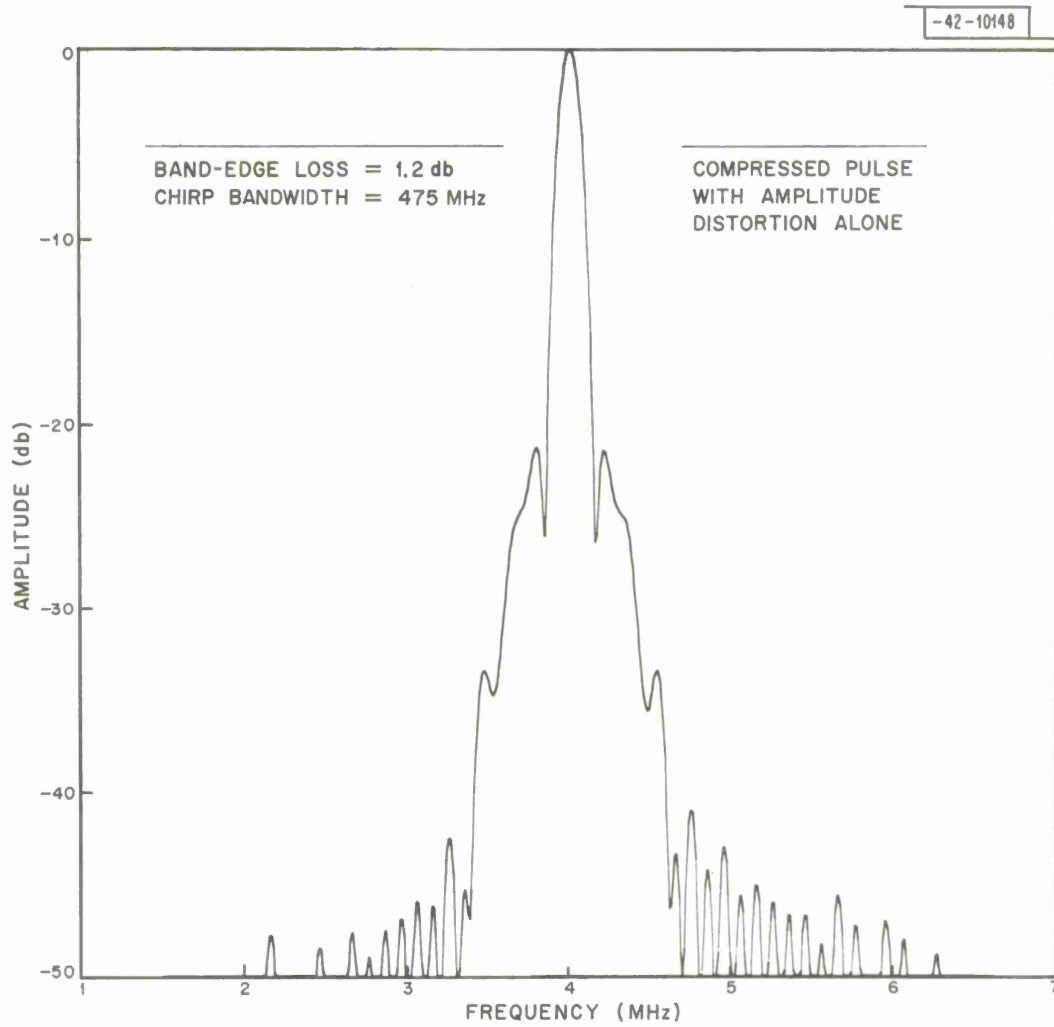Fig. 8. Matched filter output.

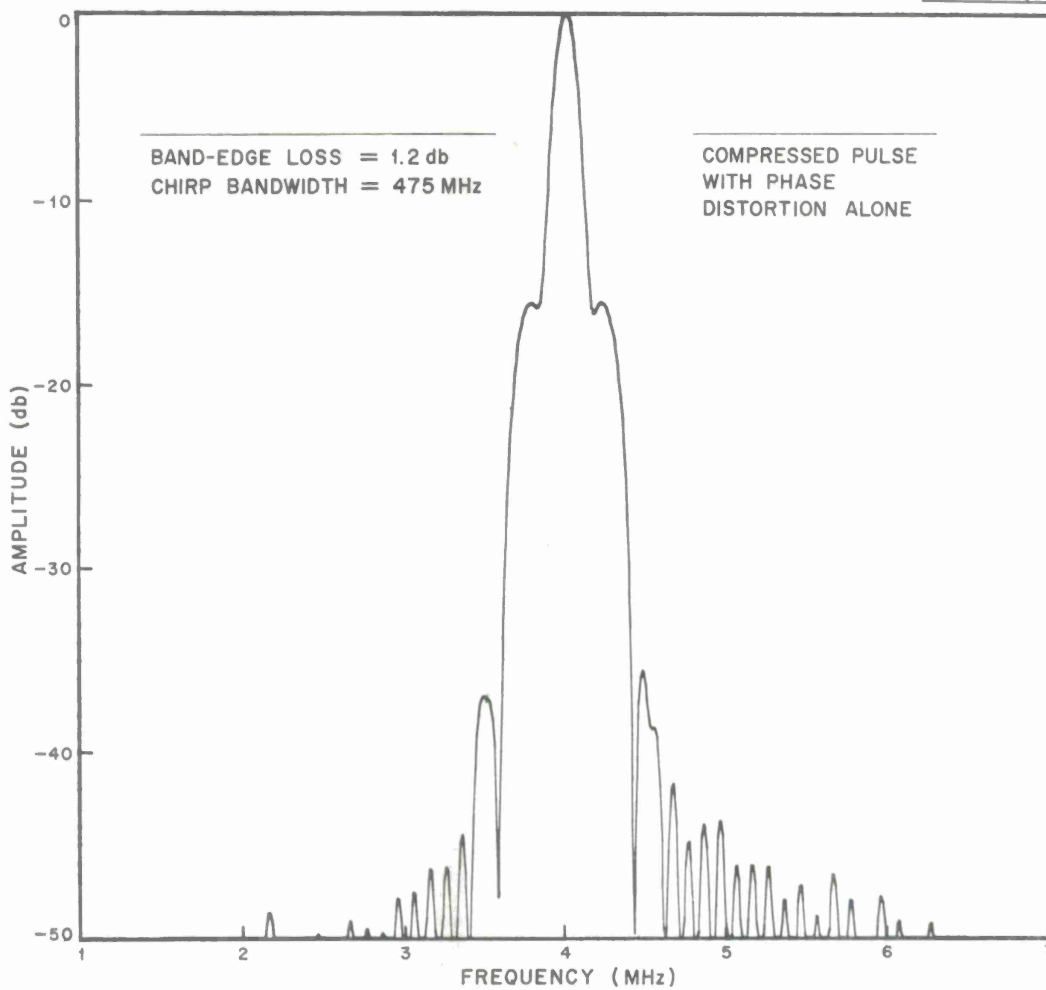16

Fig. 9. Matched filter output.

17

BAND-EDGE LOSS = 1.2 db
CHIRP BANDWIDTH = 475 MHz

COMPRESSED PULSE
WITH AMPLITUDE
AND PHASE DISTORTION

AMPLITUDE (db)

FREQUENCY (MHz)
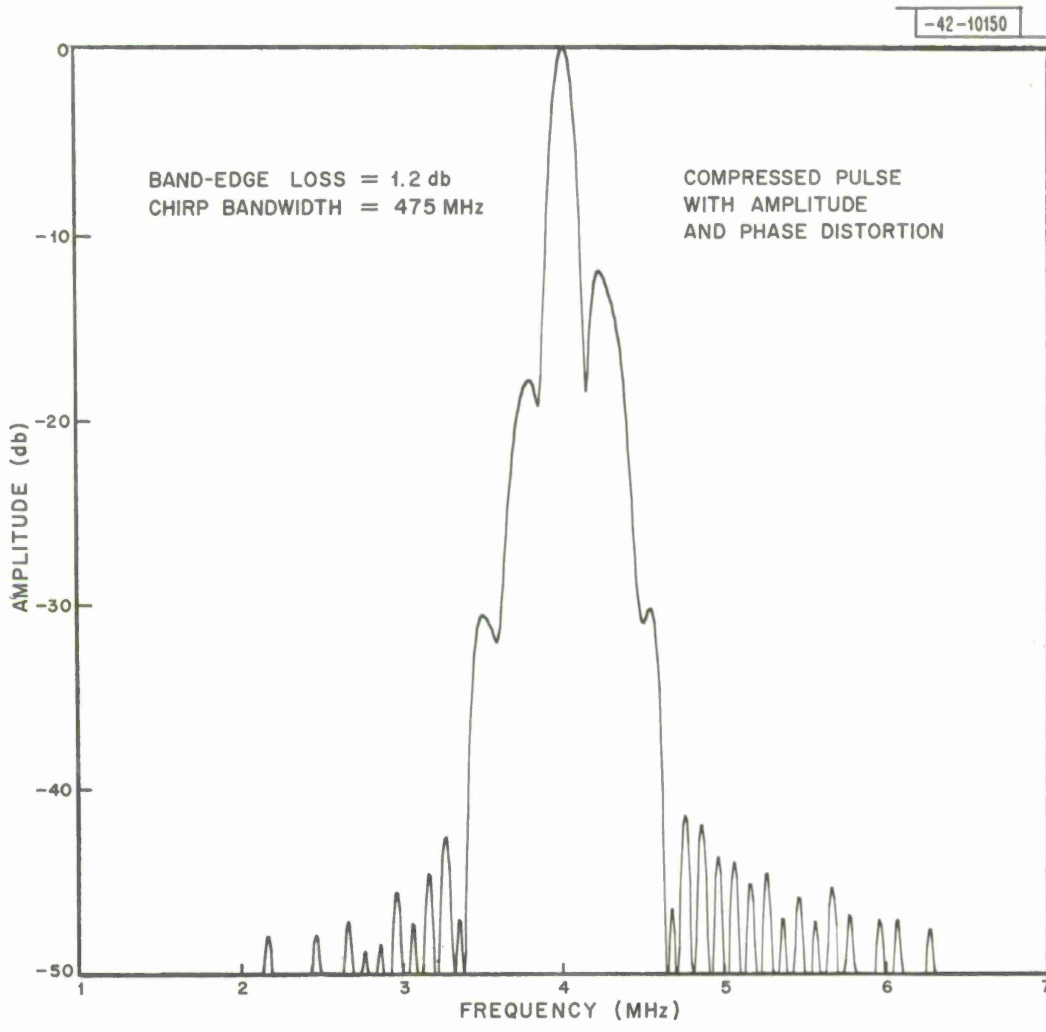
Fig. 10. Matched filter output.

18

APPENDIX A

Paired-Echo Theory

The well-known results of paired-echo theory are briefly summarized here, in a generalized form that is particularly useful in the present study.

Suppose that a system function is given by

$$H(f) = A(f) e^{j B(f)}$$

in which

$$A(f) = \begin{cases} a_0 + \sum_{n=1}^{\infty} \left[a_n \cos \frac{2n\pi f}{W} + b_n \sin \frac{2n\pi f}{W} \right], & -\frac{W}{2} \le f \le +\frac{W}{2} \\ \\ 0, & \text{elsewhere} \end{cases}$$

and

$$B(f) = c_0 + \sum_{n=1}^{\infty} \left[c_n \cos \frac{2n\pi f}{W} + d_n \sin \frac{2n\pi f}{W} \right], \quad -\frac{W}{2} \le f \le +\frac{W}{2}$$

(Note that the coefficients b_n and c_n above would vanish in the case of a realizable linear filter, but are included here for generality.)

As the first step, assume all the coefficients in the sums above are zero, except the coefficients with $n = k$. Using the expansion

$$e^{j a \cos \varphi} = J_0(a) + 2 \sum_{\ell=1}^{\infty} (j)^{\ell} J_{\ell}(a) \cos \ell \varphi$$

and the approximations (to first order in a)

$$J_0(a) \cong 1$$

19

$$J_1(a) \cong \frac{a}{2}$$

$$J_n(a) \cong 0, \ n \geq 2$$

we may write

$$e^{j \, B(f)} \cong e^{j \, c_o} \left[1 + j \, c_k \cos \frac{2k\pi f}{W} \right] \left[1 + j \, d_k \sin \frac{2k\pi f}{W} \right]$$

Writing out the product $A(f) \ e^{j \, B(f)}$, and dropping all terms of second and higher order in the (small) quantities a_k, b_k, c_k, and d_k, we arrive at the expression

$$H(f) \cong a_o \, e^{j \, c_o} \left[1 + \rho_{1k} \, e^{j \left(\gamma_{1k} + \frac{2k\pi f}{W} \right)} + \rho_{2k} \, e^{j \left(\gamma_{2k} - \frac{2k\pi f}{W} \right)} \right]$$

where

$$\rho_{1k} = \frac{1}{2} \sqrt{ \left(d_k + \frac{a_k}{a_o} \right)^2 + \left(c_k - \frac{b_k}{a_o} \right)^2 }$$

$$\rho_{2k} = \frac{1}{2} \sqrt{ \left(-d_k + \frac{a_k}{a_o} \right)^2 + \left(c_k + \frac{b_k}{a_o} \right)^2 }$$

$$\gamma_{1k} = \tan^{-1} \left[\frac{c_k - b_k/a_o}{d_k + a_k/a_o} \right] \ ; \text{ and}$$

$$\gamma_{2k} = \tan^{-1} \left[\frac{c_k + b_k/a_o}{-d_k + a_k/a_o} \right]$$

Clearly, then, if the input signal is some arbitrary complex function $f(t)$, the output can be written as

$$f_o(t) = a_o e^{j c_o} \left[f(t) + \rho_{1k} e^{j \gamma_{1k}} f(t + \tfrac{k}{W}) + \rho_{2k} e^{j \gamma_{2k}} f(t - \tfrac{k}{W}) \right] \quad ,$$

a replica of the input signal plus a pair of small leading and lagging echoes of the input signal.

Returning to the general case in which all the coefficients in $A(f)$ and $B(f)$ may be non-zero (but all are assumed <u>small</u> except a_o and c_o), it is a simple matter of book-keeping to verify that, to first order, a signal $f(t)$ transmitted through $H(f)$ can be written as

$$f_o(t) = a_o e^{j c_o} \left[f(t) + \sum_k \rho_{1k} e^{j \gamma_{1k}} f(t + \tfrac{k}{W}) + \sum_k \rho_{2k} e^{j \gamma_{2k}} f(t - \tfrac{k}{W}) \right]$$

where, for each value of k, the coefficients $\rho_{1k}, \rho_{2k}, \gamma_{1k}, \gamma_{2k}$ are defined exactly as before.

APPENDIX B

Analytic Model for a Klystron in a CHIRP System

I. Block Diagram and Description of Model

Figure B-1 is a block diagram of a proposed klystron model similar to that used in the computer simulation, whose components are so defined that the model and its implications can be analyzed mathematically.

The amplitude-phase coupling block is discussed in Section II below, but temporarily ignored in Sections III and IV, where the phaseless soft limiter and the linear filter are discussed.

It is shown that the model leads to specific predictions of spurious time sidelobes at its output, corresponding to the measured amplitude and phase data, saturation curve, and input amplitude-output phase coupling of a klystron. Furthermore, it is shown that a transversal equalizer preceding the klystron gives rise to predictable paired-echo configurations at the output of the model.

II. The Amplitude-Phase Coupling

A saturated klystron, while maintaining constant output amplitude as input level is increased, exhibits non-linear coupling between input amplitude and output phase.

This phenomenon is to be modeled as a "black box" whose output contains an additive phase term $\theta(t)$, a function of the input level. Assume that this coupling function, as measured for some representative klystron, can be adequately approximated over a suitable range by three terms of a Taylor series:

$$\theta(t) \cong k_o + k_1 A(t) + k_2 [A(t)]^2$$

where $A(t)$ is the amplitude of the input signal. If the input is an undistorted CHIRP signal, then $\theta(t)$ is merely a constant. Suppose, however, that the input signal has a single pair of echoes, at $\Delta t = \pm \frac{n}{W}$ seconds, due to a transversal equalizer; in this case, the signal can be written in the form
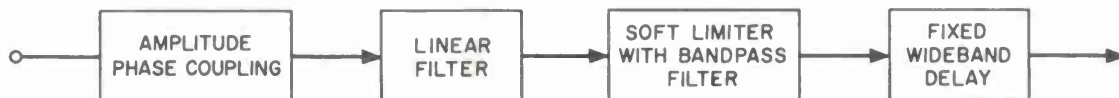
| AMPLITUDE PHASE COUPLING | → | LINEAR FILTER | → | SOFT LIMITER WITH BANDPASS FILTER | → | FIXED WIDEBAND DELAY | → |

Fig. B-1.   Klystron model.

$$e_1(t) \;=\; \left[1 + a \cos \frac{2n\pi t}{T}\right] \; \cos 2\pi \left(f_c t + \frac{Wt^2}{2T} + b \sin \frac{2n\pi t}{T}\right)$$

The additive phase term $\theta(t)$ at the output, computed from the coupling equation above, has the form

$$\theta(t) \;=\; c_1 \sin \left(\frac{2n\pi t}{T} + \varphi_1\right) \;+\; c_2 \sin \left(\frac{4n\pi t}{T} + \varphi_2\right) \;+\; \varphi_3$$

where the constants c_1, c_2, φ_1, φ_2, and φ_3 are easily determined.

It is clear that the output signal still has a pair of echoes at $\pm \frac{n}{W}$ seconds, but with modified amplitudes and phases. In addition, there are echoes at $\pm \frac{2n}{W}$ seconds, with amplitudes proportional to the (small) coefficient k_2 in the above expression for $\theta(t)$.

This result can be extended with little effort to show that each pair of echoes in a more complex TE-modified signal gives rise to two pairs of echoes at the phase-amplitude coupler's output, with the relationship described above.

At the cost of considerable labor, these altered paired echoes can be followed through the linear filter and soft limiter described in the next sections. The important point is that specific transversal equalizer settings at the model's input lead to precisely predictable paired echoes at the output. (Note that one would not ordinarily be interested in actually making these predictions. In using a TE in a radar system, one adjusts the TE by trial and error until the sidelobe structure in the receiver compressed pulse is visually optimized.)

III. The Phaseless Soft Limiter

In Chapter 2 of Middleton, Introduction to Statistical Communication Theory, (McGraw-Hill, New York, N.Y., 1960) there is an excellent treatment of a technique for analyzing a device with the following characteristics:

$$y \;=\; y(t) \;=\; \text{input}$$
$$z(t) = g(y) \;=\; \text{output}$$

$$
g(y) = \begin{cases} \beta \, y^{1/\nu} & , \quad y > 0 \\ -\beta \, |y|^{1/\nu} & , \quad y < 0 \end{cases}
$$

A representative $g(y)$ is shown in Fig. B-2.

One may model an idealized soft limiter with such a device, if the input $y(t)$ is suitably restricted in magnitude (since the magnitude of the device output $z(t)$ does not asymptotically approach a constant). The free parameter ν is to be chosen to give a good fit to the measured saturation curve of a klystron.

The limiter characteristic may be broken into two parts,

$$
g_+(y) = \begin{cases} 0 & , \quad y < 0 \\ g(y) & ; \quad y > 0 \end{cases} \quad , \text{ and}
$$

$$
g_-(y) = \begin{cases} g(y) & , \quad y < 0 \\ 0 & ; \quad y > 0 \end{cases}
$$

in order to obtain its two-sided complex Fourier transform:

$$
f(ju) = \int_0^\infty g_+(y) \, e^{-j \, u \, y} \, dy]_{\text{Im } u < 0}
$$

$$
+ \int_{-\infty}^0 g_-(y) \, e^{-j \, u \, y} \, dy]_{\text{Im } u > 0}
$$

$$
= f_+(ju) + f_-(ju)
$$

Note that, because $g(-y) = -g(y)$, we need retain only $f_+(ju)$, and we may write the inverse transform as

$$
g(y) = \frac{j}{\pi} \int_C f_+(ju) \sin(uy) \, du
$$

25

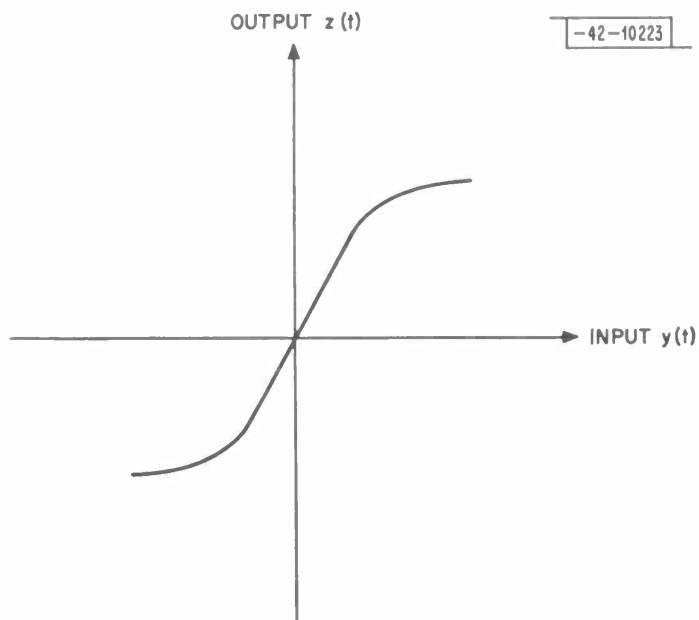OUTPUT z (t)

—42—10223

INPUT y(t)

Fig. B-2.   Phaseless soft limiter model characteristic.

26

Carrying out the transformation for the limiter characteristic $g(y)$ above, we find

$$f_+(ju) = \frac{\beta \, \Gamma(\frac{1}{\nu} + 1)}{(ju)^{\frac{1}{\nu} + 1}}$$

where the u-plane contour C for the inverse transformation is the entire real axis, with a semicircular indentation below the origin.

Let $y(t)$ be a CHIRP signal with possible amplitude and phase modulation,

$$y(t) = A(t) \cos[\omega_c t + \Phi(t) + \varphi]$$

where ω_c is the carrier frequency. Substituting this expression for y in the inverse-transform equation above, and using the expansion

$$\sin(a \cos \varphi) = \sum_{\text{odd } \ell} (-1)^{(\ell-1)/2} \, 2 \, J_\ell(a) \cos \ell \, \varphi$$

we have

$$z(t) = g(y) = \sum_{\text{odd } \ell} B_\ell(t) \cos \ell[\omega_c t + \Phi(t) + \varphi]$$

where

$$B_\ell(t) = \frac{j(-1)^{(\ell-1)/2}}{\pi} \int_C f_+(ju) \, J_\ell[u \, A(t)] \, du$$

and $J_\ell(a)$ is the Bessel function of the first kind, ℓ^{th} order. Thus $z(t)$ contains all odd-order harmonics of the input signal.

If the limiter is followed by a suitable low-pass filter one obtains

$$z_1(t) = B_1(t) \cos [\omega_c t + \Phi(t) + \varphi]$$

$B_1(t)$ can be evaluated, using an equation on page 121 of Middleton; the result is

$$B_1(t) = \beta K_1(\nu) [A(t)]^{1/\nu}$$

Thus the final output has the same phase as the input CHIRP signal, but the amplitude modulation has been raised to the $1/\nu$ power and multiplied by a constant.

IV. Combination of the Linear Filter and Soft Limiter

The paired-echo theory summarized in Appendix A provides a convenient means for dealing with the distorted phase and amplitude characteristics of a klystron, visualized as a linear filter preceding the soft limiter model.

Initially, suppose the amplitude and phase characteristics of a particular klystron were so simple that they could each be represented by a single (small) Fourier component. The corresponding linear filter, with a unit amplitude CHIRP input $y(t)$, would produce an output signal

$$y_1(t) = y(t) + a_1 y(t-\tau) + a_2 y(t+\tau)$$

We now repeat the soft limiter analysis in Section III above, using $y_1(t)$ as the input to the limiter, and making approximations to first order in the small parameters a_1 and a_2. Thus we assume, for example, that

$$J_0(a_1) \cong 1 \quad ,$$

$$J_1(a_1) \cong \frac{1}{2} a_1 \quad ,$$

$$J_n(a_1) \cong 0 \quad , \quad \text{all } n \geq 0$$

which are essentially the same approximations made in deriving paired-echo theory. The resulting sequence of calculations, while quite straightforward, is very

23

lengthy; only the results are stated here. In effect, the output of the low-pass filter following the limiter is

$$z_1(t) \cong \beta\, b_o\, [y(t) + \epsilon_1\, |a_1|^{1/\nu}\, y(t-\tau)$$

$$+ \epsilon_2\, |a_2|^{1/\nu}\, y(t+\tau)]$$

where the constant

$$b_o = \frac{j}{\pi} \int_C J_1(u)\, f(ju)\, du$$

$$= \frac{\Gamma(\frac{1}{\nu} + 1)}{2^\nu\, \Gamma[\frac{1}{2}(\frac{1}{\nu} + 1)]\, \Gamma[\frac{1}{2}(\frac{1}{\nu} + 3)]}$$

and ϵ_1 and ϵ_2 are unit-magnitude constants whose signs correspond to the original signs of a_1 and a_2.

Thus $z_1(t)$ still has paired echoes at $\pm\, \tau$ seconds, but with increased amplitudes relative to the main lobe (since $|a|^{1/\nu} > |a|$, if $|a| < 1$ and $\nu > 1$.

This result is readily generalized to the more realistic case in which the linear filter (representing klystron phase and amplitude distortion) requires many Fourier components for adequate descriptions of its magnitude and phase. As we have seen, paired echo theory predicts that, with an input $y(t)$, the filter output will have the form

$$y_1(t) = y(t) + \sum a_k\, y(t - \tau_k) + \sum b_k\, y(t + \tau_k)$$

to first order in all the a_k and b_k, which are assumed to be small.

The details of determining the soft limiter model's output are omitted here, for the sake of brevity. The task is a straightforward but very tedious matter of plugging $y_1(t)$ into the analysis in Section III above, writing out all the expressions and cross products, and dropping all terms of higher than

29

first order in the a_k and b_k, with the simple and intuitively satisfying result that the output is given by

$$z_1(t) \cong \beta\, b_o \left[y(t) + \sum \epsilon_{ak} \left| a_k \right|^{1/\nu} y(t - \tau_k) \right.$$
$$\left. + \sum \epsilon_{bk} \left| b_k \right|^{1/\nu} y(t + \tau_k) \right]$$

in which b_o has the value given above, and the ϵ_{ak} and ϵ_{bk} again serve to carry along the original signs of the a_k and b_k.

Observe that each echo at the limiter input has a corresponding echo at the limiter output, with the same time displacement, but somewhat increased amplitude.

Digital Low-Pass Filter

An elegant tool for the design of digital computer algorithms to simulate linear filters, the Z-transform, is treated in detail in Lincoln Laboratory Technical Note 1965-63, "Digital Filter Design Techniques", by Rader and Gold. Basically, the Z-transform is the digital analog of the Laplace transform in linear systems theory.

An ordinary differential equation, considered in the context of sampled time functions and digital approximations, becomes a difference equation, whose solution can be attacked by means of the Z-transform, defined as

$$F(Z) = \sum_{n=0}^{\infty} f(nT) \, Z^{-n}$$

where T is the sampling interval. For a linear filter one defines a system function $H'(Z)$, related to the Z-transform $H(Z)$ of the filter's impulse response $h(t)$ by the equation

$$H'(Z): \quad \frac{F_{out}(Z)}{F_{in}(Z)} = T \, H(Z)$$

The extra factor T above is explained by noting that a unit impulse $u_o(t)$ should be represented by a single sample of height $\frac{1}{T}$ (equivalent to a rectangular pulse of height $\frac{1}{T}$ and width T, with unit area). Since one actually represents an impulse by a single sample of unit height, the system function must be multiplied by T.

For the particular application in the present study, a digital realization was desired for a filter with s-plane system function

$$H(s) = \frac{a^3}{(s + a)^3}$$

which is equivalent to the cascade of three sub-filters

$$H_c(s) \ = \ \frac{a}{s + a}$$

The impulse response of the sub-filter is

$$h_c(t) = \begin{cases} 0 & , \quad t < 0 \\ a \, e^{-at} & , \quad t \geq 0 \end{cases}$$

whose Z-transform is

$$H_c(Z) = \sum_{n=0}^{\infty} a \, e^{-anT} \, Z^{-n} = \sum_{n=0}^{\infty} a(e^{-aT} \, Z^{-1})^n = \frac{a}{1 - e^{-aT} \, Z^{-1}}$$

from which we obtain the system function

$$H_c'(Z) \ = \ \frac{aT}{1 - e^{-aT} \, Z^{-1}}$$

Writing

$$H_c'(Z) \ = \ \frac{F_{out}(Z)}{F_{in}(Z)}$$

(where $F_{out}(Z)$ and $F_{in}(Z)$ are the sub-filter output and input), and solving for $F_{out}(Z)$, we find

$$F_{out}(Z) \ = \ aT \, F_{in}(Z) + e^{-aT} \, Z^{-1} \, F_{out}(Z)$$

From the definition of the Z-transform, we find that a delayed time function

$$g(t - T)$$

has the transform

$$Z^{-1} \, G(Z)$$

where $G(Z)$ is the transform of $g(t)$.

Thus we find that the digital realization of the desired filter has the form shown in Fig. C-1
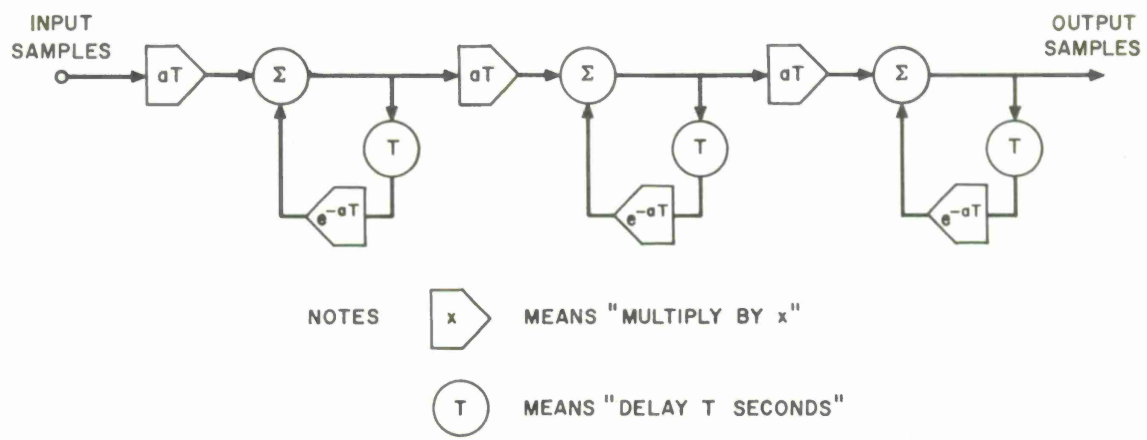
INPUT
SAMPLES

OUTPUT
SAMPLES

NOTES ⬠x MEANS "MULTIPLY BY x"

Ⓣ MEANS "DELAY T SECONDS"

Fig. C-1. Digital realization of three-pole filter.

34

Distribution:

Division IV

    J. Freedman
    G. F. Watson
    H. G. Weiss

Group 42

    M. E. Austin
    A. Bertolini
    D. R. Bromaghim
    G. F. Dalrymple
    D. F. DeLong
    A. A. Galvin
    H. M. Heggestad (5)
    H. F. Hoffman (3)
    E. M. Hofstetter
    B. Loesch
    J. Margolin
    G. R. McCully
    J. P. Perry
    C. M. Steinmetz
    J. Tabaczynski
    J. O. Taylor

Group 43

    L. B. Anderson
    R. C. Butman
    M. P. Fraser
    G. L. Guernsey
    P. A. Ingwersen
    W. A. Janvrin
    J. G. Jelatis
    P. B. McCorison
    G. B. Morse
    E. Silverman

Group 45

    M. Axelbank
    W. A. Both
    W. W. Camp
    W. H. Drury
    B. H. Labitt
    D. F. Mayer
    C. J. McKenney
    S. J. Miller
    W. B. Renhult
    R. G. Sandholm
    R. W. Straw
    J. H. Teele

DOCUMENT CONTROL DATA - R&D

(Security classification of title, body of abstract and indexing annotation must be entered when the overall report is classified)

1. ORIGINATING ACTIVITY (Corporate author)	2a. REPORT SECURITY CLASSIFICATION
Lincoln Laboratory, M.I.T.	Unclassified
	2b. GROUP None

3. REPORT TITLE

A Preliminary Study of Klystron Distortion in a CHIRP Radar System

4. DESCRIPTIVE NOTES *(Type of report and inclusive dates)*

Technical Note

5. AUTHOR(S) *(Last name, first name, initial)*

Heggestad, Harold M.

6. REPORT DATE	7a. TOTAL NO. OF PAGES	7b. NO. OF REFS
28 December 1966	40	2

8a. CONTRACT OR GRANT NO. AF 19 (628)-5167	9a. ORIGINATOR'S REPORT NUMBER(S)
b. PROJECT NO. ARPA Order 498	Technical Note 1966-54
c.	9b. OTHER REPORT NO(S) *(Any other numbers that may be assigned this report)*
d.	ESD-TR-66-602

10. AVAILABILITY/LIMITATION NOTICES

Distribution of this document is unlimited.

11. SUPPLEMENTARY NOTES	12. SPONSORING MILITARY ACTIVITY
None	Advanced Research Projects Agency, Department of Defense

13. ABSTRACT

A study has been made of the effects of klystron saturation, and phase and amplitude distortion, on the performance of a wideband high-power CHIRP radar system. Mathematical analysis of a general non-linear model for a klystron indicates that satisfactory operation of the radar system can still be achieved in the face of the grossly non-ideal character of the tube, with suitable restrictions, if appropriate compensation is applied. Extraneous paired echoes in the signal at the klystron input (whether present because of previous distortion, or deliberately introduced by a transversal equalizer) are shown to have a specific relationship with paired echoes at the klystron output.

A FORTRAN computer program has been written to simulate the performance in a CHIRP system of any suitable klystron (or other high-power amplifier tube, such as a twystron or TWT). The inputs to the program include measured tube data, such as the CW amplitude versus frequency and phase versus frequency characteristics and the input versus output saturation curve. The user of the program specifies what he feels is the usable bandwidth of the tube. The program simulates a pure CHIRP signal of that bandwidth and delivers plots of the weighted compressed pulse that would appear at the receiver output.

In addition, by inspection of the output compressed pulse plots, one can estimate transversal equalizer settings to cancel the spurious sidelobes, introduce the equalized CHIRP pulse into the program in place of the former undistorted input, and observe the degree of compensation in the output pulse.

The report includes reproductions of the output plots generated by the simulation program, for a representative set of klystron data.

14. KEY WORDS

radar	CHIRP	klystrons